


The effect of pre-treatment on the production of lignocellulosic nanofibers and their application as a reinforcing agent in paper

Eduardo Espinosa · Juan Domínguez-Robles · Rafael Sánchez · Quim Tarrés · Alejandro Rodríguez 

Received: 3 October 2016 / Accepted: 28 March 2017 / Published online: 3 April 2017
© Springer Science+Business Media Dordrecht 2017

Abstract In this work, three different lignocellulosic nanofibers (LCNF) were produced from unbleached wheat straw soda pulp by using different pre-treatments: mechanical, enzymatic, and TEMPO [(2,2,6,6-tetramethylpiperidin-1-yl) oxy radical]-mediated oxidation processes. The different LCNF were characterized and studied by their chemical composition (FTIR), crystal structure (XRD), thermal degradation behaviour (TGA), morphological (TEM), and their reinforcement effect on papermaking slurries. The pre-treatment used to obtain LCNF showed significant differences on the nanofibrillation yield (37–95%), carboxyl content ($74\text{--}362\ \mu\text{mol g}^{-1}$), cationic demand ($428\text{--}1116\ \mu\text{eq g}^{-1}$), and on its dimensions (7–14 nm), thermal stability, and structure. Regarding application as reinforcement on papermaking slurries, LCNF obtained by TEMPO-mediated oxidation produced a greater reinforcing effect than the other LCNF. Nevertheless, the obtained LCNF from mechanical process produce a similar

increase in the mechanical properties of the paper-sheets due to its high length, compared with LCNF obtained by TEMPO-mediated oxidation.

Keywords Wheat straw · TEMPO · Enzymatic · Mechanical · Isolation · Characterization

Introduction

In the near future, bio-economy should become the engine that drives the advancement of developed and developing countries. To reach this objective, one of the main vectors must be research into effectiveness and efficiency of exploitation of natural resources, with the ultimate objective to maximise their use entirely and, therefore, generate the least possible amount of residue. The lignocellulosic materials constitute a very heterogeneous set of raw materials in origin and composition (all sharing the prevalence of lignin and cellulose as fundamental constituents), subject to be fully exploited. In recent decades, cellulosic fibers from lignocellulosic biomass have been researched for application in multiple industry sectors such as construction industry, paper and cardboard industry, biomedicine, etc. (Lu et al. 2014; Mohammadzemi et al. 2009). Thus, to supply such growing demand, it is necessary to research non-wood cellulosic raw materials, such as fast-growing annual plants and waste from agricultural activity (Vargas et al. 2012; Feria et al. 2012).

E. Espinosa · J. Domínguez-Robles · R. Sánchez · A. Rodríguez (✉)
Chemical Engineering Department, Faculty of Science,
University of Córdoba, Building Marie-Curie, Campus of
Rabanales, 14014 Córdoba, Spain
e-mail: a.rodriguez@uco.es

Q. Tarrés
Group LEPAMAP, Department of Chemical Engineering,
University of Gerona, c/M. Aurèlia Campmany, no. 61,
17071 Gerona, Spain

Cereal straw is an example of agricultural waste susceptible for use. World cereal production in 2015 was close to 2530 million tons, 30% (736 million tons) of which was wheat (FAO 2016). Considering that for every 1 kg of grain, approximately 1 kg of residue in the form of straw is generated (Rodríguez et al. 2010), in 2015 736 million tons of wheat straw was produced, which may be used for the production of cellulosic fibers.

Cellulose nanofibers (CNF) offer a huge potential in the design of new materials and properties. This is due to the nanometric size of the fibers, which gives them different properties than those present in their original size. CNF obtained from the disintegration of cellulosic pulps have long length and small diameter, also presenting good stiffness values and the ability to form networks through secondary bonds, including hydrogen bonds (Benhamou et al. 2014).

The first CNFs were obtained by Turbak et al. (1983), by submitting wood cellulose pulp suspension to high shearing and impact forces, passing it through a high pressure homogenizer several times getting a cellulosic fiber suspension with 25–100 nm diameter.

The most effective method for the production of CNF in the range of 3–10 nm was developed by Saito et al. (2007). The method consists of a chemical pre-treatment of the pulp (TEMPO-mediated oxidation) causing an electrostatic repulsion due to the induction of negative charges on the carboxylate groups at the surface of the fibrils.

The enzymatic hydrolysis of cellulose has also been used as pre-treatment prior to homogenization using β -1,4-endoglucanases, which randomly hydrolyze accessible intramolecular β -1,4-glucosidic bonds in cellulose chains exposing the individual cellulose polysaccharide chains (Henriksson et al. 2007; Pääkkö et al. 2007). The production of CNF is also possible through exclusive use of mechanical treatments, using as pre-treatment a high mechanical beating to individualize the fibers before homogenization (Yousefi et al. 2011; Afra et al. 2013).

In the field of nanotechnology, the CNF effect on conventional paper has been studied by many authors (González et al. 2012; Delgado-Aguilar et al. 2014). The addition of CNF as additive for paper improves the permeability and tensile index of papers due to the increment of the number of hydrogen bond fibril-fibers (Kajanto and Kosonen 2012). The increase of paper strength due to CNF addition can be compared with

strength improvement after a light refining (González et al. 2012).

The addition of CNF to unrefined pulp produces papersheets with higher tensile strength than standard papersheets, allowing significant grammage reduction and energy savings (refining processes) (Vallejos et al. 2016).

The morphology and properties of cellulose nanostructures produced by the aforementioned treatments are different. For this reason, it is necessary to study the effect that different pre-treatments produce in the production of CNF, to know the final physical and chemical characteristics of nanofibers and optimize its use and application (Yousefi et al. 2011). Using cellulosic pulps obtained from wheat straw through soda pulping process, as this process is the most effective for LCNF isolation from wheat straw (Sánchez et al. 2016), this work aims to analyse the effect of the different pre-treatments (mechanical process, TEMPO-mediated oxidation, and enzymatic hydrolysis) on the production of cellulose nanofibers, as well as the reinforcement effect on eucalyptus bleached kraft paper strength.

Materials and methods

Raw materials

The raw material used in this work, wheat straw, was provided by Ecopapel S.L. enterprise from Seville, Spain. Regarding the raw material preparation and chemical characterization, a previous work was considered (Espinosa et al. 2016). Bleached kraft hardwood pulp (BKHP) was used as a standard substrate and was kindly supplied by Ence-Celulosas (Navia, Spain).

Pulp and lignocellulosic nanofibers isolation

Delignification process

The delignification process of the wheat straw was made using the same operational conditions [100 °C, 150 min, 7% soda (over dry matter), and liquid/solid ratio of 10:1] as in a previous work (Espinosa et al. 2016). The characterization of the dried pulp was determined using the following methods, beating degree (TAPPI T-227), yield (gravimetric method),

α -cellulose (T-9m54), lignin (T-203os61), holocellulose (T-222), ash (T-211), ethanol extractable (T-204), Kappa number (T-236cm85), and viscosity (T-30om94).

TEMPO pre-treatment (TO-LCNF)

The procedure and reagent ratios used by Besbes et al. (2011a) were applied for TEMPO-mediated oxidation of cellulose fibers. A 10 ± 0.1 g sample of wheat soda pulp was suspended in 500 mL distilled water containing TEMPO (0.16 g) and NaBr (1 g). TEMPO-mediated oxidation was started adding 12% NaClO solution (5 mmol) with continuous stirring at room temperature. The pH was maintained at 10 by adding 0.5 M NaOH using a pH stat until no NaOH consumption was observed (reaction time ≈ 2 h). After the end of the oxidation reaction, 100 mL of ethanol was added, and the oxidized fibers were filtered and washed several times with distilled water. After that, a 1% aqueous suspension of these oxidized fibers was passed through a high pressure homogenizer in order to avoid seals in the equipment.

Mechanical pre-treatment (Mec-LCNF)

The lignocellulosic nanofibers were obtained by mechanical pre-treatment beating the wheat soda pulp (28 °SR) in a PFI beater (Metrotec) according to ISO 5264-2:2002 until achieving a drainage rate of 90°SR. Then, a 1% aqueous suspension was prepared and passed through a high pressure homogenizer.

Enzymatic pre-treatment (Enz-LCNF)

An enzymatic pre-treatment (biobeating) was used followed by a high pressure homogenization to obtain LCNF. The enzymatic hydrolysis was performed using the commercial enzyme cocktail Novozym 476, kindly provided by Novozymes A/S (Denmark), which contains 2% endo- β -1,4-glucanases with an activity factor of 4500 CNF-CA/g cellulose (tested over a CMC substrate). The enzymatic reaction was carried out for 3 h on 75 g of wheat soda pulp suspended in a 1.5 L of pH 5 buffer at 50 °C, using a 0.83% enzyme dosage based on the dry weight of the pulp. At the end of the reaction time, the suspension was heated to 80 °C for 15 min in order to denature the enzyme and stop the pre-treatment. The obtained

fibers were filtered and washed several times with distilled water. Then, a 1% aqueous suspension was prepared and passed through a high pressure homogenizer.

High pressure homogenization

Once the pulp was brought under the different pre-treatments, it was passed through a high pressure homogenizer (PANDA GEA 2 K NIRO). The homogenization was realized following the sequence described by Espinosa et al. (2016).

Papersheets production and characterization

Increasing amounts (0–5%, 1% increments) of lignocellulose nanofibers (LCNF) from the different pre-treatments were added and mixed on bleached kraft hardwood pulp (BKHP) by means of a pulp disintegrator with the following operation conditions: 3000 rpm during 60 min and 1.5% consistency. This methodology has been used in previous works and has proved to be effective in improving the dispersion of CNF in papermaking slurries (Alcalá et al. 2013; González et al. 2013; Delgado-Aguilar et al. 2015). After this step, a 1% solution of cationic starch (Vector SC 20157) and colloidal silica (LUDOX[®] HS-40 colloidal silica) were added at 0.5 and 0.8% expressed on dry BKHP, respectively. The application of these retention agents was done at soft agitation of the suspension at 1% consistency for 30 min. This step is necessary in order to avoid LCNF loss during the dewatering process because the equipment is not able to retain nanometric material. The LCNF presents an anionic charge; therefore, a cationic element is needed to be used as microparticle retention system (Xu et al. 2013). Different types of retention agents have been studied to analyze their effectiveness in the retention of cellulose nanofibers. Taipale et al. (2010) investigated the effect that different types of CNF have on the drainage of kraft pulp and the strength of papers produced, using cationic polychloride (poly-DAD-MAC), cationic starch, and three different types of polyacrylamides (C-PAM). The use of cationic starch as retention agent has been used to retain nanocrystalline cellulose (NCC) in the application in deinked pulp (Xu et al. 2013). In that study, two retention systems were investigated, cationic polyacrylamide (CPAM/NCC) and cationic starch (CS/

NCC). These retention systems increased the retention of NCC on pulp without affecting the drainage value in papersheets. The use of these retention systems can promote the occurrence of fiber flocs, thus affecting the uniformity of the sheet and, therefore, the performance of paper. To avoid this problem, colloidal silica is used as deflocculant to prevent floc formation and avoid problems during sheet formation. The negatively charged particles of colloidal silica have a great interaction with the positive surfaces of the fibers, once the cationic starch is added and retain on the fibers, and this interaction avoids the formation of fiber flocs, making the distribution of fiber in the sheet much better. The retention system used in this work has been studied and widely used in literature (Alcalá et al. 2013; Delgado-Aguilar et al. 2014; Espinosa et al. 2016; Tarrés et al. 2016). Papersheets with LCNF content (from 0 to 5% over dried material) were fabricated in a sheet former (ENJO-F-39.71) according to ISO standard 5269-2 and conditioned in a weather chamber at 25 °C and 50% humidity for 48 h before the mechanical test was performed.

Once conditioned, the basis weight, as well as their physico-chemical characteristics were determined following ISO standards (ISO 536, 1924-1, 1924-2, 1974, and 2758).

Characterization

Yield of nanofibrillated cellulose

The LCNF suspension was centrifuged in order to separate the unfibrillated part from the partially fibrillated materials. The protocol was carried out as described in the bibliography (Besbes et al. 2011a): A 0.1 wt% solid content suspension (S_c) was centrifuged at 4500 rpm for 30 min to separate the nanofibrillated material (in the supernatant fraction) from the non-fibrillated or partially fibrillated fractions, which settled out. The sediments were dried to a constant weight at 100 °C. The yield was calculated from the next equation:

$$\text{Yield \%} = \left(1 - \frac{\text{Weight of dried sediments}}{(\text{Weight of diluted sample} \cdot \%SC)} \right) \cdot 100 \quad (1)$$

Optical transmittance

The optical transmittance is an indirect indicator of the nanofibrillation yield (Delgado-Aguilar et al. 2016; Meng et al. 2016). The LCNF suspensions were introduced into a quartz cuvette, and the transmittance was measured from 400 to 800 nm using a Lambda 25 UV-Spectrometer. The spectrum of a cuvette filled with distilled water was used as the reference.

Carboxyl content

The carboxyl content (CC) of the different LCNF was determined using conductometric titration, as described in Besbes et al. (2011a). The LCNF samples (15 mg dried weight) were suspended into 15 mL of 0.01 M HCl solution. After stirring for 30 min, the suspension was titrated with 0.05 M NaOH. The titration curves showed three characteristics regions with two intersection points (V_1 and V_2) corresponding the first regions to the excess of HCl, the second corresponds to the volume of NaOH required to neutralize the weak acidic (carboxylic) groups, and the third region corresponds to the NaOH excess. The volume of NaOH (L) used in the second region is used to determine the carboxyl content of the fibers.

$$CC = \frac{162(V_2 - V_1) \cdot c}{w - 36(V_2 - V_1) \cdot c} \quad (2)$$

where c is the concentration of the sodium hydroxide (mol L^{-1}) solution and w is the oven-dry weight of cellulose (g). The results indicate the average mmols of $-\text{COOH}$ groups per gram of LCNF.

Cationic demand

The cationic demand was determined by means of a Mütek PCD 05 particle charge detector, following the methodology described by Espinosa et al. (2016) through the next equation:

$$CD = \frac{(C_{\text{Poly-D}} \cdot V_{\text{Poly-D}}) \cdot (V_{\text{Pes-Na}} \cdot C_{\text{Pes-Na}})}{w} \quad (3)$$

where CD is the cationic demand ($\mu\text{eq g}^{-1}$), $C_{\text{Poly-D}}$ = cationic polymer concentration (1 meq L^{-1}), $C_{\text{Pes-Na}}$ = anionic polymer concentration (1 meq L^{-1}),

$V_{\text{Poly-D}}$ = used volume of cationic polymer and $V_{\text{Pes-Na}}$ = used volume of anionic polymer and w = sample's dry weight.

Degree of polymerization

The degree of polymerization of cellulose chains forming pulp and LCNF can be estimated from the average intrinsic viscosity value (Tanaka et al. 2014). For cellulose, the intrinsic viscosity (η_s in mL g⁻¹) is related to the degree of polymerization (DP) and empirical relationship is suggested following the next equations (Marx-Figini 1987):

$$\text{DP}(<950) \quad \text{DP} = \left[\frac{\eta_s}{0.42} \right] \quad (4)$$

$$\text{DP}(>950) \quad \text{DP}^{0.76} = \left[\frac{\eta_s}{2.28} \right] \quad (5)$$

The analyses were performed dissolving pulp and LCNF in cupriethylenediamine (1 N) as the solvent. For each sample, three measurements of the efflux time at the same concentration have been realized to determine the intrinsic viscosity at 25 ± 0.1 °C.

Specific surface and diameter estimation

Several authors explain two possible mechanisms that could be involved in the interaction between CNF and poly-DADMAC (Rouger and Mutjé 1984; Carrasco et al. 1998), (1) ionic interaction between the cationic polymer and the carboxylic groups on the cellulose surface and (2) surface interactions due to London-Van der Waals forces. Both mechanisms could be assumed to occur at the same time forming poly-DADMAC in a single layer. In this case, by estimating the specific surface area of a single poly-DADMAC molecule, it is possible to calculate theoretically the specific surface of LCNF, and finally, considering a cylindrical geometry for LCNF, it is possible to calculate their average diameter.

Field emission scanning electron microscopy (FE-SEM)

In order to corroborate the accuracy of the diameter calculation, nanopapers from the different LCNF were

prepared by casting and observed through FE-SEM. Nanopaper was fixed to the substrate with double-sided tape and metalize with a 10 nm gold layer before observation. The size and morphology of the coated nanofibers were examined by field emission scanning electron microscopy (FE-SEM) in a S-4700 microscope (Hitachi, Japan).

FTIR analysis

The effect of the pre-treatments on chemistry structure of LCNF was examined by FTIR. Infrared spectra were obtained on a FTIR-ATR Perkin-Elmer Spectrum Two collecting 20 scans from 450 to 4000 cm⁻¹ with a resolution of 4 cm⁻¹. Analysis was performed on pulp dried in an air oven at 60 °C for 24 h and NFC films prepared by heat-drying of LCNF suspensions.

Thermogravimetric analysis (TGA)

The thermal stability of the pulp and the different samples of LCNF were determined by TGA measurements performed using a Mettler Toledo Thermogravimetric analyser (TGA/DSC 1). The amount of sample used for each measurement was 10.0 ± 1.0 mg. All measurements were performed under nitrogen atmosphere with a nitrogen gas flow of 50 mL min⁻¹ by heating the samples from room temperature to 900 °C at a heating rate of 10 °C min⁻¹.

X-ray diffraction (XRD)

The XRD Spectra for soda pulp and the different LCNF were collected on a Bruker D8 Discover with a monochromatic source Cu K α 1. The LCNF were freeze-dried and compressed into flat sheets with the thickness of around 1 mm before measurement. Diffractograms were recorder over an angular range of 7°–50° at a scan of 1°/38.4 s. The crystallinity index (CI) was calculated from the intensity of the 2 0 0 peak (I_{200} $2\theta = 22^\circ$) and the intensity minimum (I_{am} between the peaks at 2 0 0 and 1 1 0 (I_{100} $2\theta = 15^\circ$) by using the empirical equation (Segal et al. 1959):

$$\text{CI} = \frac{I_{200} - I_{\text{am}}}{I_{200}} \cdot 100 \quad (6)$$

Results and discussion

Wheat straw fibers

Table 1 shows the results obtained from the chemical characterization of wheat straw compared with other raw materials used in obtaining LCNF found in the literature.

The comparison of raw materials underscores that wheat straw could be used for the production of LCNF, such as the other raw materials, due to the high α -cellulose and hemicellulose content that it has. Moreover, the lower lignin content of wheat straw compared to the rest, facilitates the efficient production of LCNF by the three processes mentioned (TEMPO-mediated oxidation, mechanical process, and enzymatic hydrolysis). In general, for a TEMPO-mediated oxidation, a low lignin content allows the use of oxidative power in the oxidation of cellulose instead of in the oxidation of lignin. In the mechanical process, the effectiveness of mechanical beating increases because during the beating the fiber swelling is reduced by the presence of lignin for its hydrophobic character which harm the water absorption of the fibers. Last, in the enzymatic hydrolysis, high lignin content avoids the unfolding of cellulose chains hindering the enzyme accessibility.

After the pulping process the content of α -cellulose in pulp increases (from 39.7 to 59.20%) and the lignin and ash content decreases (from 17.7 and 7.72% to 13.31 and 2.47%, respectively). As for the hemicellulose content, a slight decrease occurs (from 30.6 to 25.71%), despite this, a higher content remains compared with other pulp used in LCNF production, such as *Cladophora glomerata* (15.3%) and those obtained from bark residue (15.3%) (Nair and Yan 2015; Xiang et al. 2016).

The hemicellulose content plays a key factor in the nanofibrillation because hemicelluloses act as inhibitors of the coalescence of microfibrils and facilitate the nanofibrillation (Iwamoto et al. 2008). The polymerization degree obtained (1630) indicates a high fiber length.

Characterization and morphology of CNF

The nanofibers obtained by TEMPO-mediated oxidation have a higher nanofibrillation yield than the ones obtained by mechanical process and enzymatic hydrolysis (Table 2).

The light transmittance is wavelength-dependent and it is related to nanofiber size due to the Rayleigh scattering effect (Meng et al. 2016). The light scattering, therefore, depends on the size of the dispersed nanofibrils, so if the LCNF presents a bigger size, it scatters more light, resulting in a lower transparency degree (Besbes et al. 2011b). Then, this parameter can be used as an indirect indicator of nanofibrillation yield of LCNF suspensions due to lower nanofibrillation yield result in a high light scattering compared with those suspensions which have a high nanofibrillation yield causing a lower light scattering. The carboxylate groups amount also affects the stability and transparency of nanocellulose suspension as a result by the electrostatic repulsion among the nanofibrils (Meng et al. 2016). Due to the synergy of these parameters, TO-LCNF presents the highest value followed by those obtained by a mechanical process and last, those obtained by enzymatic hydrolysis.

The cationic demand is calculated for the absorption of a cationic polymer (poly-DADMAC) onto the LCNF surface. The cationic demand is related to two parameters, (1) the specific surface of the fiber and (2)

Table 1 Raw material characterization

	Ash (%)	α -cellulose (%)	Hemicellulose (%)	Lignin (%)	References
Wheat straw	7.72	39.7	30.6	17.7	
Cotton stalks	1.8	40.1	25.7	30.9	Soni et al. (2015)
Eucalyptus sawdust	0.59	41.8	10.7	32.3	Vallejos et al. (2016)
Rapeseed straw	6.5	44	31	21	Chacker et al. (2014)
Rice straw	19	41	31	24	Chacker et al. (2014)
Corn straw	7.5	40.8	34	22	Chacker et al. (2014)

Table 2 LCNF Characterization

LCNF	Yield (%)	Transmittance (%)	Cationic demand ($\mu\text{eq g}^{-1}$)	Carboxyl content ($\mu\text{mols g}^{-1}$)	Specific surface ($\text{m}^2 \text{g}^{-1}$)	Diameter (nm)	Degree of polymerization (DP)
TO-LCNF	>95	<90	1116	362.4	367.01	6.81	502
Mec-LCNF	55.6	<75	441	<74.4	178.53	14.01	1395
Enz-LCNF	37.45	<40	428	<74.4	172.20	14.52	931

the number of carboxyl groups, so an increase in this demand is associated with an increase in the specific surface of the fiber or an increase in the carboxyl groups content.

Because TEMPO-mediated oxidation produces nanofibers with a very small diameter and presents a higher carboxyl content (Besbes et al. 2011a; González et al. 2014; Delgado-Aguilar et al. 2015), the cationic demand is much higher than the nanofibers obtained by other processes, since it is close to $1200 \mu\text{eq g}^{-1}$, similar to the values described in literature (González et al. 2014). Regarding the carboxyl content, the Mec-LCNF and Enz-LCNF have a value of $74.4 \mu\text{eq g}^{-1}$. However, nanofibers obtained by TEMPO-mediated oxidation have a higher carboxyl content because of oxidation augment the amount of carboxylate groups on the surface of the fiber (Benhamou et al. 2014; Besbes et al. 2011b; Saito and Isogai 2004).

Regarding diameter, smaller diameter nanofibers are obtained using TEMPO-mediated oxidation as pre-treatment compared to mechanical and enzymatic pre-treatments. Nevertheless, the oxidation results in fiber degradation as indicated by the values obtained for the degree of polymerization, since this is highest in the nanofibers obtained by mechanical process where less fiber degradation occurs compared to chemical and enzymatic pre-treatment.

Figure 1 shows nanometric size for the different LCNF, presenting similar diameter in Enz-LCNF and Mec-LCNF, and a smaller diameter in those nanofibers obtained by TEMPO-mediated oxidation (TO-LCNF), adjusting to the results obtained by the theoretical estimate.

Fourier transform-infrared spectroscopy (FTIR) analysis

Figure 2 shows the FTIR spectrum for wheat straw soda pulp and the different cellulose nanofibers. The

spectral bands at 3300 and 2845 cm^{-1} correspond to O–H and C–H stretching vibration of $\text{CH}_2\text{–OH}$ groups of cellulose structure (Moran et al. 2008). Despite analysing the dried samples, the peak detected at 1743 cm^{-1} in Enz-LCNF corresponds to O–H bending of absorbed water during the test (Tian et al. 2016). TEMPO-mediated oxidation converts selectively the C6 primary hydroxyls of cellulose into C6 sodium carboxylate groups, for this reason, the peak at 1604 cm^{-1} , assigned to C=O stretching in carboxyl groups, is more prominent in TO-LCNF (Jiang and Hsieh 2013). This is corroborated by the higher carboxyl content present in TO-LCNF compared to the rest of LCNF. The peak at 1510 cm^{-1} correspond to aromatic ring vibrations related with the lignin content in soda pulp, Mec-LCNF, and Enz-LCNF, but it is not present in TO-LCNF due to lignin oxidation during the pre-treatment and, therefore, fiber bleaching (Ibrahim et al. 2013). The peaks at 1370 , 1162 , and 1110 cm^{-1} correspond to C–H vibrations, glycosidic bonds (C–O–C) and C–OH, respectively (Xiang et al. 2016). The intense peak at 1600 cm^{-1} is due to C–C stretching related with the cellulose structure (Moran et al. 2008).

X-ray diffraction analysis

The crystalline structure of cellulose is well studied using the XRD patterns. Two characteristic peaks are present in all the patterns at around 22° and $15^\circ 2\theta$ angles, attributed to the diffraction planes of (101) and (002), which commonly represent typical cellulose I crystal form (Bettaieb et al. 2015). The ordered crystalline arrangements in the celluloses appears due to the formation of inter- and intramolecular H-bonding by the hydroxyl groups (Chirayil et al. 2014). The H-bonding restricts the free movement of the cellulosic chains, and the chains align close together in an orderly manner, which tends to have

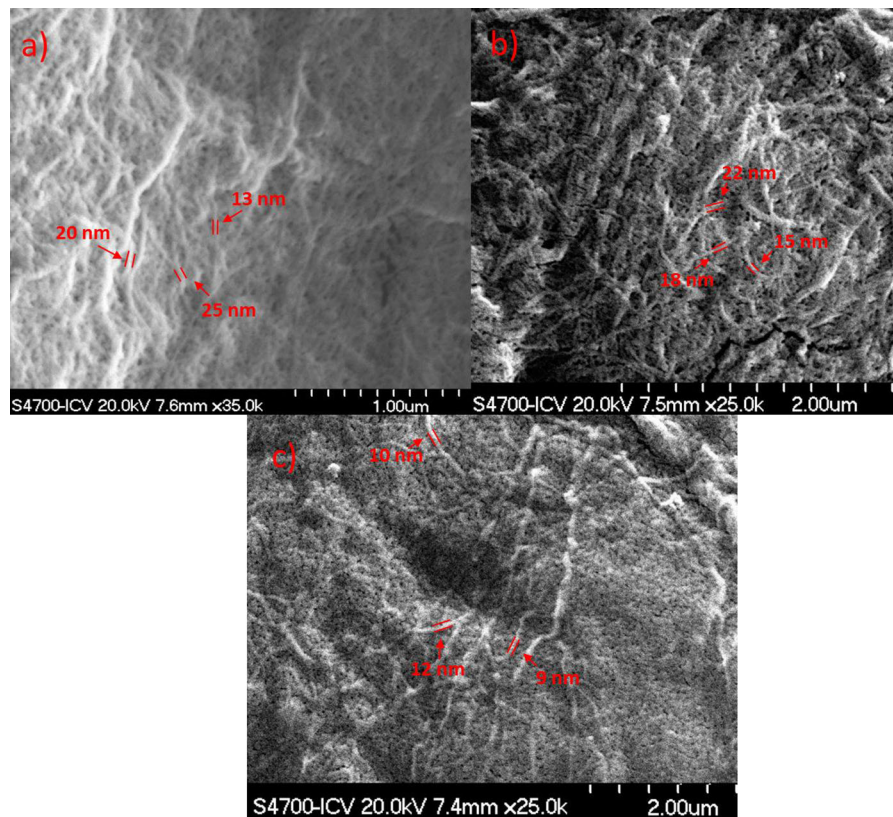


Fig. 1 Nanopapers FE-SEM microphotography: **a** Enz-LCNF, **b** Mec-LCNF, and **c** TO-LCNF

the crystallinity. Unlike in nanocrystalline cellulose, where the amorphous regions have been destroyed, the crystalline domains in the lignocellulose nanofibers are embedded in the matrix of amorphous components such as hemicellulose, lignin, and pectin, thus a low crystallinity is shown. Figure 3 shows XRD patterns of soda pulp and the different LCNF, which was used to evaluate the effect of pre-treatment on crystallinity. Soda pulp presents a low crystallinity associated with the presence of amorphous components such as hemicellulose, lignin, and pectin (Chandra et al. 2016). This value is lower in unbleached pulps compared to bleached pulps due to the removal of lignin. Compared to the original fibers (soda pulp), the LCNF samples present lower values of CI due to the pre-treatment and to high pressure homogenization. Each pre-treatment has a different effect on the cellulose crystalline domains. The decrease in the CI of TEMPO-oxidized cellulose could be explained by the fact that almost all carboxyl groups formed by the

oxidation are present on the surfaces of crystalline cellulose microfibrils (Tanaka et al. 2012) and by the sodium glucuronosyl units that lead to convert some crystalline regions of cellulose into disordered structures during the oxidation reaction (Puangsins et al. 2013). In the case of Mec-LCNF, a depth beating produces that the crystalline index of the samples decreased due to a high beating intensify the forces action on crystalline regions of cellulose, resulting in a higher disordering of these regions.

In the case of Enz-LCNF, a slight decrease in the CI is observed, associated with the shear forces which they are subjected to during the homogenization process (Iwamoto et al. 2007). Despite all LCNF suffer the effect of high pressure homogenization process, those obtained from mechanical beating as pre-treatment resulting in a higher disordering of crystalline regions than those obtained from enzymatic hydrolysis.

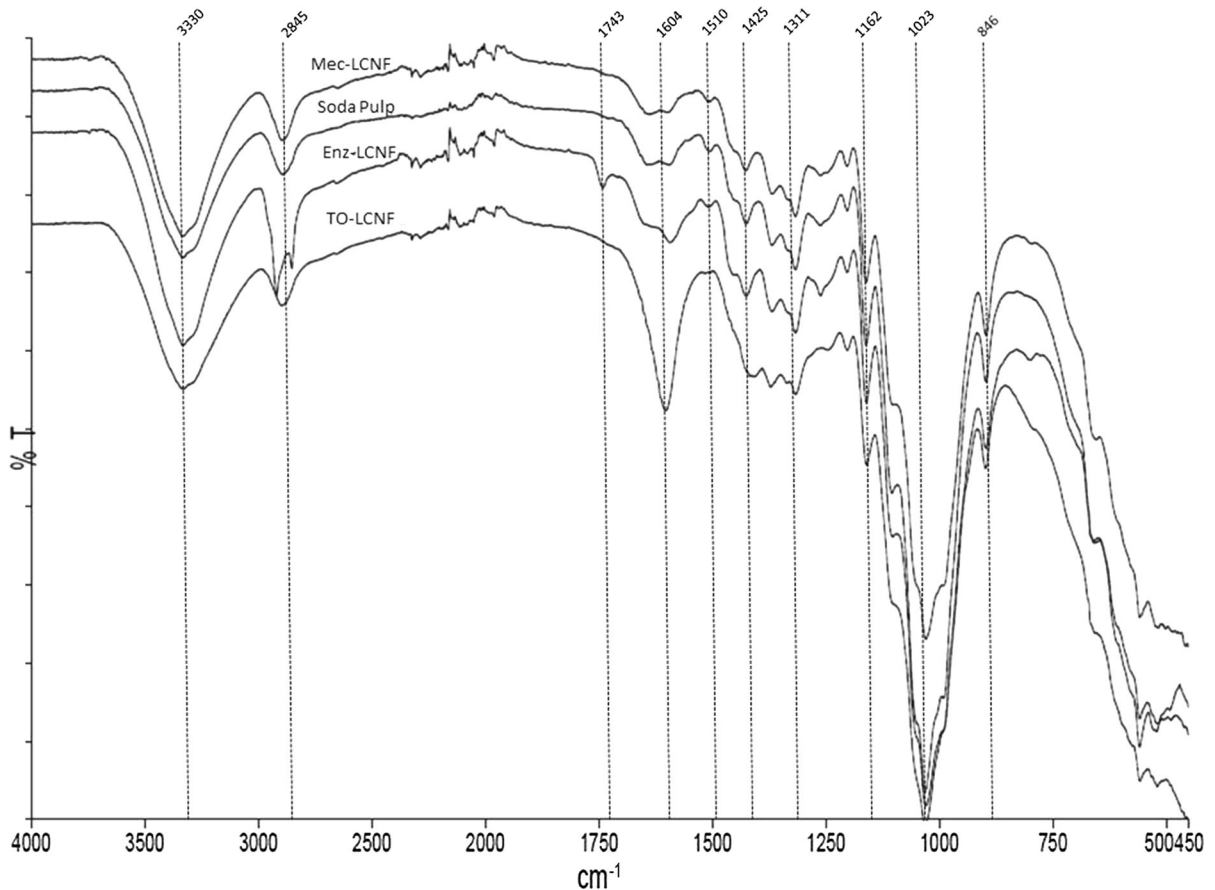


Fig. 2 FTIR Spectrum of Mec-LCNF, soda pulp, Enz-LCNF, and TO-LCNF

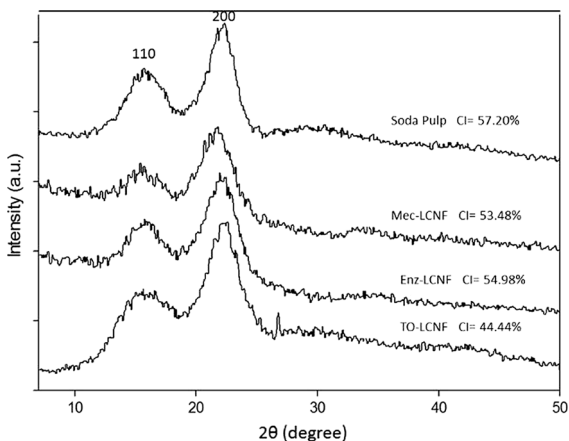


Fig. 3 XRD patterns of soda pulp, Mec-LCNF, Enz-LCNF, and TO-LCNF

Thermogravimetric analysis

The thermal stability and degradation behaviour of LCNF is an important parameter for the application in biocomposite processing (Abdul Khalil et al. 2012). The TGA weight loss curve and the derivative of the weight loss curve with temperature (dm/dT) were analysed to obtain results of thermogravimetric analysis of soda pulp, TO-LCNF, Mec-LCNF, and Enz-LCNF as shown in Fig. 4. A slight weight loss is observed in the range of 30 to 200 °C in all TGA weight loss curves due to evaporation of absorbed and intermolecular H-bonded water. In the 250–400 °C range the greatest weight loss occurs in all the samples due to the breaking of glycosidic bonds, pyrolysis reactions of polysaccharides, dehydration, and

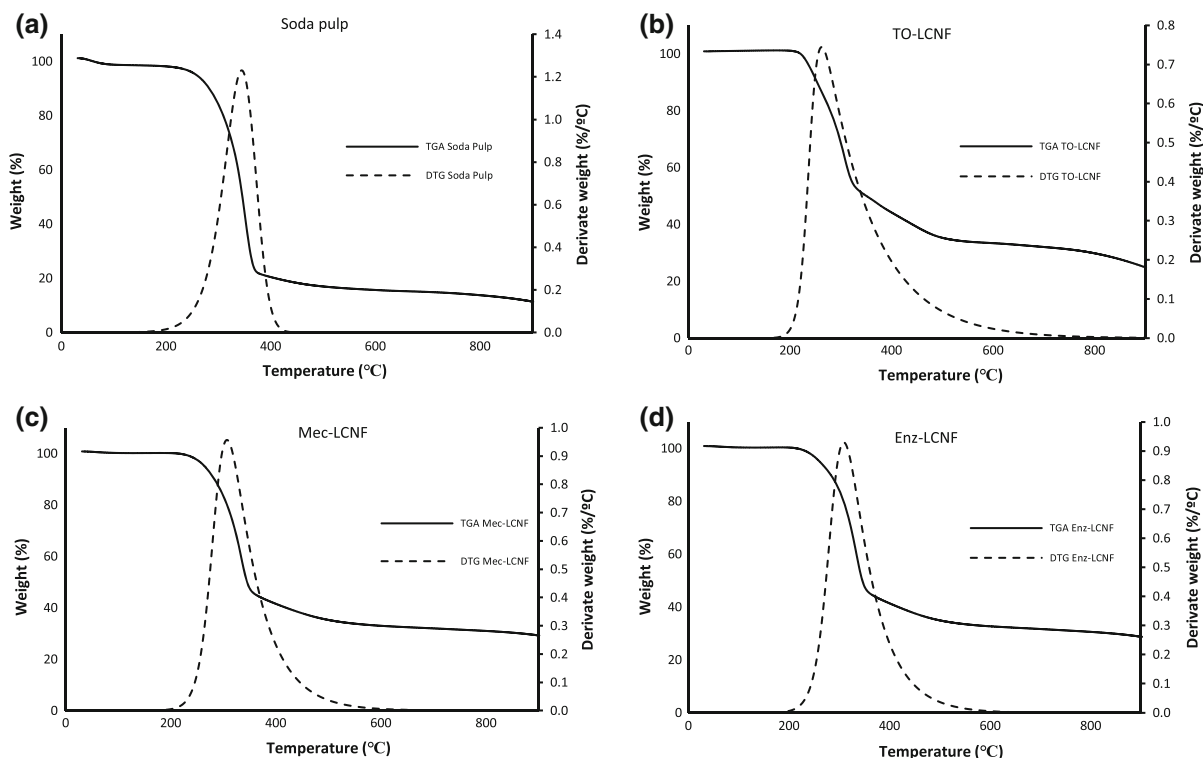


Fig. 4 TGA and DTG curves of **a** soda pulp, **b** TO-LCNF, **c** Mec-LCNF, and **d** Enz-LCNF

depolymerisation, with production of low molecular weight compounds and formation of charred residue to occur under nitrogen atmosphere (Tian et al. 2016).

As described in the literature, the thermal stability of LCNF is lowest compared to larger size cellulosic fibers (Quiévy et al. 2010; Nair and Yan 2015). When LCNF are exposed to heat, due to its higher specific surface begin to discompose faster than those with a lower specific surface and higher diameter (Tian et al. 2016). The T_{max} values of samples refers to the maximum value of the derivate weight loss denoting the temperature at which the degradation rate is fastest, are 345, 263, 307, and 309 °C for soda pulp, TO-LCNF, Mec-LCNF, and Enz-LCNF, respectively. It is noted that TO-LCNF, which has a considerably smaller diameter than other LCNF, reaches the maximum value of degradation at lower temperature than the other LCNF, followed by Mec-LCNF and finally Enz-LCNF. As Table 2 shows, the order regarding temperature where the maximum degradation values are reached, are in agreement with the order from smallest to largest size diameter obtained for the different LCNF. On the other hand, the

crystallinity of the fiber affects their thermal stability, so it relates that those presenting higher CI as LCNF obtained by mechanical process and enzymatic hydrolysis show a higher thermal stability that those that present low CI such as those obtained from TEMPO-mediated oxidation. The worse thermal stability of TO-LCNF could be also explained that because of their higher carboxyl content, they present a larger number of free ends, thus affecting the thermal stability of the nanofibers (Sharma and Varma 2014).

Reinforcement effect on papermaking slurries

With a larger specific surface and a higher charge density, the ability of the fiber to form bonds with other fibers is higher, thereby increasing the strength of papersheets. Because of this feature, LCNF are perfect candidates to be used as reinforcement in papermaking slurries as a replacement step for mechanical beating. It is unclear what effect the cationic starch has on the mechanical properties of the papersheets when it is added as retention agent. To determine this effect, the effect of the retention system

without LCNF addition was studied, and it showed that the mechanical properties increase reaching a maximum value of 18–20%. Determining that most of the reinforcement effect is produced by adding LCNF. The strengthening contribution of LCNF to papersheets properties may be explained through two possible mechanisms; in the first one, LCNF act as an adhesion promoter by bridging adjacent fibers and favouring the fiber–fiber bonding, increasing the bonded area; in the second one, LCNF may generate a different network embedded among larger fibers that contributes to boost the load-bearing capacity of the paper (Boufi et al. 2016).

To check the viability of the usage of wheat straw LCNF as a reinforcement agent in papermaking slurries, the evolution of physical properties of the papersheets was studied by adding them on bleached kraft hardwood pulp (Fig. 5).

As expected, the addition of LCNF increased the strength properties of papersheets, but it was shown that the isolation conditions of the LCNF samples have much influence in its application as reinforcement, due to their differences in size and surface charge. The breaking length, tear index, and burst index were all improved with the addition of LCNF.

The largest increase in the different physical properties is produced by the addition of TO-LCNF due to its higher specific surface, increasing the relative bonded area and improving the physical properties of papersheets. Regarding the reinforcement effect of the LCNF, from a content of 3% LCNF (except for Mec-LCNF) an asymptotic value is reached where a further increase is not achieved for the physical properties values. This effect is due to this relative bonded area and cannot be further increased at a certain point, which leads to a stagnation of the physical properties improvement (Tarrés et al. 2016).

Although TO-LCNF produces a greater increase, the Mec-LCNF, despite its larger diameter, has a higher length as is observed in the values obtained for degree of polymerization (Table 2). This higher length promotes a better crosslinking with the rest of the fibers, thereby improving the physical properties of papersheets in similar values to those obtained by the addition of TO-LCNF. However, LCNF produced by enzymatic pre-treatment present a similar diameter to those obtained mechanically, but with a significantly smaller length. Because of these parameters, the improvement in physical properties of papersheets

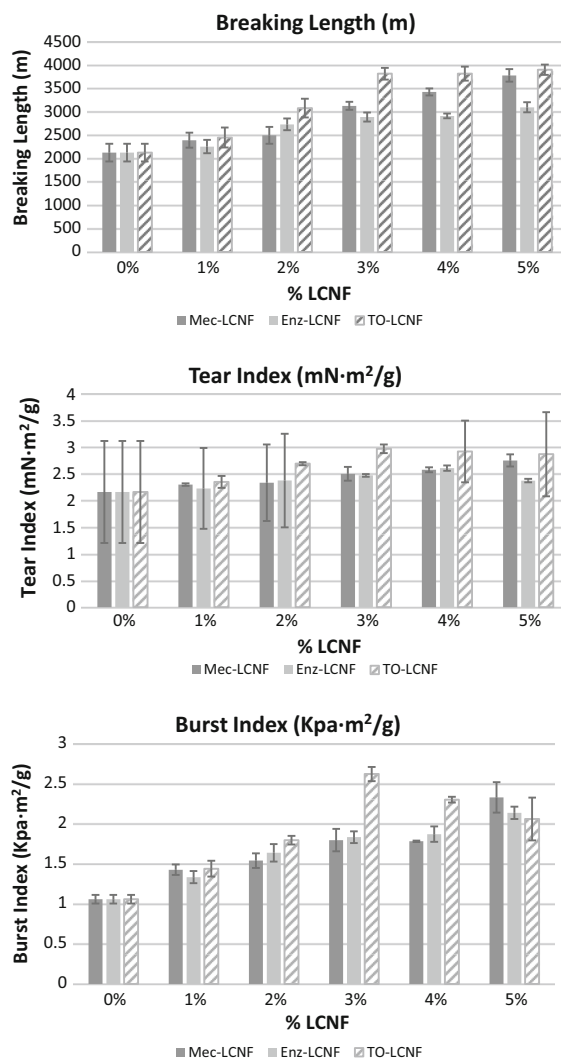


Fig. 5 Evolution of the mechanical properties of BKHP with different amounts of LCNF

does not reach high values compared with the other LCNF used in this work.

The drainage properties of the papermaking slurries are of key importance in the papermaking processes, because if the drainage is too slow, the retention time of the papermaking slurries during the dewatering process is increased, thus affecting the capacity of production. The large specific surface of the LCNF and, therefore, the high amount of hydroxyl groups on nanofiber's surface, bind water increasing the retention values, causes the viscosity of the fibrous suspensions to increase and reduces the drainage rate, despite the low added amounts of LCNF. The fact that

the addition of LCNF on papermaking slurries increased Schopper Riegler Degree ($^{\circ}\text{SR}$) has been reported previously by several works (Delgado-Aguilar et al. 2016; Vallejos et al. 2016).

The drainage properties evolution of BKHP papermaking slurries reinforced with ascending amounts of the different LCNF are shown in Fig. 6. The graph shows how the increase in the Schopper Riegler Degree ($^{\circ}\text{SR}$) produced by the Mec-LCNF and Enz-LCNF is less than the increase produced by TO-LCNF. This phenomenon is due to the higher charge density and carboxyl content, which produce a greater water binding to the fiber compared to those that present a lower charge density and carboxyl content. Therefore, the use of Mec-LCNF as reinforcement agent produces similar values of reinforcement, and in turn, produces a lower increase in the $^{\circ}\text{SR}$, damaging to a lesser extent the papermaking process compared to TO-LCNF.

In view of the results, it can be concluded that TO-LCNF have the greatest reinforcement capacity of the three LCNF studied. Nevertheless, if the cost of obtaining the different LCNF is considered, the TO-LCNF have an estimated cost of 206€/kg (Delgado-Aguilar et al. 2015), due to the high price of reagents used in the oxidation process, mainly TEMPO catalyst, because even nowadays, no successful methodology has been reported to recover the TEMPO catalyst at an industrial scale. By contrast, Enz-LCNF needs a lower investment to be produced, 13.71€/kg (Delgado-Aguilar et al. 2015), but the process requires greater control (pH and temperature) to promote a proper operation for the pre-treatment. In this case, the buffering agents represent a great part of the final cost to obtain this type of LCNF. Finally, for those LCNF

obtained by mechanical pre-treatment a final cost of 2.55€/kg is needed (Espinosa et al. 2016), almost 100 times less than for those obtained by TEMPO-mediated oxidation and five times less than those obtained by enzymatic hydrolysis. The costs to obtain LCNF by enzymatic hydrolysis and mechanical pre-treatment are much lower, so these types of LCNF are presented as an economically viable alternative for use as reinforcement on papermaking slurries, especially Mec-LCNF, which despite its low cost with a 5% LCNF content, reaches a reinforcement effect just 5.7% lower than the achieved with TO-LCNF. Its high specific surface and his great length facilitate the crosslinking of nanofibers with the other fibers during the papersheets formation allowing an increase similar to that obtained by TO-LCNF despite its larger diameter.

Therefore, Mec-LCNF are good candidates for use as industrial-scale reinforcement to improve physical properties of papersheets due to their low cost and simple production process. This technology would be particularly relevant as a substitute for mechanical beating in the recycling process of paper and cardboard, because the traditional refining process involves, generally, a loss of physical–mechanical fiber properties due to the physical modification that it produces, so if this modification is avoided, the number of recycling cycles that the original fibers can endure increases.

Conclusions

Wheat straw soda pulp was used to isolated lignocellulose nanofibers (LCNF) using mechanical, enzymatic, and chemical pre-treatments followed by high pressure homogenization. The lignonanofibers characterization indicates that the lignonanofibers obtained by TEMPO-mediated oxidation, presents smaller diameter, but shorter lengths due to the degradation during the oxidation process than those values obtained in mechanical and enzymatic lignonanofibers. FE-SEM images were used to assure the nanometric size of the fibers. The FTIR spectrum reveals the increase in carboxyl content caused by TEMPO-oxidation. The XRD patterns of the different samples shows the decrease in the crystallinity index by the different pre-treatments, resulting a higher crystallinity index in the mechanical and enzymatic

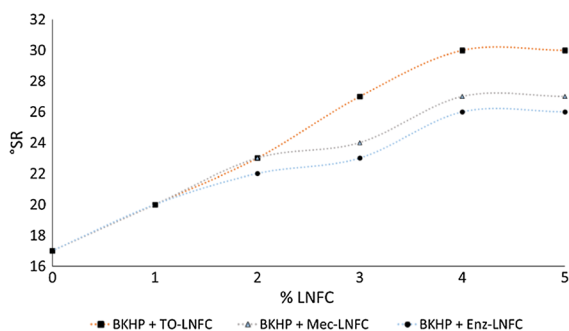


Fig. 6 Drainage properties evolution of papermaking slurries by adding different amounts LCNF

lignonanofibers. In addition, the lignonanofibers with a high crystallinity index present a higher thermal stability. The application of the LCNF as reinforcement agent on papermaking shows that, due to its high specific surface and the ability to form bonds with other fibers, increase the mechanical properties of the papersheets. This is stressed in TO-LCNF and Mec-LCNF, since the latter is cheaper than TO-LCNF to obtain similar values of reinforcement. This work provides a way to generate lignocellulose nanofibers from wheat straw soda pulp, using different pretreatments and its effective application as papermaking reinforcement.

Acknowledgments The authors are grateful to Spain's DGICYT, MICINN for funding this research within the framework of the Projects CTQ2013-46804-C2-2-R and supported by the Spanish Ministry of Science and Education through the National Program FPU (Grant Number FPU14/02278), and also to the staff of the Central Service for Research Support (SCAI) at the University of Córdoba.

References

- Abdul Khalil HPS, Bhat AH, Ireana Yusra AF (2012) Green composites from sustainable cellulose nanofibrils: a review. *Carbohydr Polym* 87:963–979
- Afra E, Yousefi H, Hadilam MH, Nishino T (2013) Comparative effect of mechanical beating and nanofibrillation on paper properties made from bagasse and softwood pulps. *Carbohydr Polym* 97:725–730
- Alcalá M, González I, Boufi S, Vilaseca F, Mutjé P (2013) All-cellulose composites from unbleached hardwood kraft pulp reinforced with nanofibrillated cellulose. *Cellulose* 20:2909–2921
- Benhamou K, Dufresne A, Magnin A, Mortha G, Kaddami H (2014) Control of size and viscoelastic properties of nanofibrillated cellulose from palm tree by varying the TEMPO-mediated oxidation. *Carbohydr Polym* 99:74–83
- Besbes I, Alila S, Boufi S (2011a) Nanofibrillated cellulose from TEMPO-oxidized eucalyptus fibers: effect of the carboxyl content. *Carbohydr Polym* 84(3):975–983
- Besbes I, Vilar MR, Boufi S (2011b) Nanofibrillated cellulose from Alfa, Eucalyptus and Pine fibers: preparation, characteristics and reinforcing potential. *Carbohydr Polym* 84:1198–1206
- Bettaieb F, Khiari R, Dufresne A, Mhenni MF, Belgacem MN (2015) Mechanical and thermal properties of *Posidonia oenica* cellulose nanocrystal reinforced polymer. *Carbohydr Polym* 123:99–104
- Boufi S, González I, Delgado-Aguilar M, Tarrés Q, Pèlach MA, Mutjé P (2016) Nanofibrillated cellulose as an additive in papermaking process: a review. *Carbohydr Polym* 154:151–166
- Carrasco F, Mutjé P, Pelàch MA (1998) Control of retention in paper-making by colloid titration and zeta potential techniques. *Wood Sci Technol* 32(2):145–155
- Cereal Supply and Demand Brief. Food and Agriculture Organization of the United Nation (FAO) (2016) <http://www.fao.org/worldfoodsituation/csdb/en/>. Accessed 30 May 2016
- Chacker A, Mutje P, Vilar MR, Boufi S (2014) Agriculture crop residues as a source for the production of nanofibrillated cellulose with low energy demand. *Cellulose* 21:4247–4259
- Chandra CS, Neena G, Sunil KN (2016) Isolation and characterization of cellulose nanofibrils from arecanut husk fiber. *Carbohydr Polym* 142:158–166
- Chirayil CJ, Joy J, Mathew L, Mozetic M, Koetz J, Thomsa S (2014) Isolation and characterization of cellulose nanofibrils from *Helicteres isora* plant. *Ind Crop Prod* 59:27–37
- Delgado-Aguilar M, González I, Pelàch MA, De la Fuente E, Negro C, Mutjé P (2014) Improvement of deinked old newspaper/old magazine pulp suspensions by means of nanofibrillated cellulose addition. *Cellulose* 22(1):789–802
- Delgado-Aguilar M, González I, Tarrés Q, Alcalá M, Pèlach MA, Mutjé P (2015) Approaching a low-cost production of cellulose nanofibers for papermaking applications. *BioResources* 10(3):5345–5355
- Delgado-Aguilar M, González I, Tarrés Q, Pèlach MA, Alcalá M, Mutjé P (2016) The key role of lignin in the production of low-cost lignocellulosic nanofibers for papermaking applications. *Ind Crops Prod* 86:295–300
- Espinosa E, Tarrés Q, Delgado-Aguilar M, González I, Mutjé P, Rodríguez A (2016) Suitability of wheat straw semi-chemical pulp for the fabrication of lignocellulosic nanofibers and their application to papermaking slurries. *Cellulose* 23:837–852
- Feria JM, Alfaro A, López F, Pérez A, García JC, Rivera A (2012) Integral valorization of *Leucaena diversifolia* by hydrothermal and pulping processing. *Bioresour Technol* 103:381–388
- González I, Boufi S, Pelàch MA, Alcalá M, Vilaseca F, Mutjé P (2012) Nanofibrillated cellulose as paper additive in eucalyptus pulps. *BioResources* 7(4):5167–5180
- González I, Alcalá M, Arbat G, Vilaseca F, Mutjé P (2013) Suitability of rapeseed chemithermomechanical pulp as raw material in papermaking. *BioResources* 8(2):1697–1708
- González I, Alcalá M, Chinga-Carrasco G, Vilaseca F, Boufi S, Mutjé P (2014) From paper to nanopaper: evolution of mechanical and physical properties. *Cellulose* 21(4):2599–2609
- Henriksson M, Henriksson G, Berglund LA, Lindström T (2007) An environmentally friendly method for enzyme-assisted preparation of microfibrillated cellulose (MFC) nanofibers. *Eur Polym J* 43(8):3434–3441
- Ibrahim MM, El-Zawawy WK, Juttke Y, Koschella A, Heinze T (2013) Cellulose and microcrystalline cellulose from rice straw and banana plant waste—preparation and characterization. *Cellulose* 20:2403–2416

- Iwamoto S, Nakagaito A, Yano H (2007) Nano-fibrillation of pulp fibers for the processing of transparent nanocomposites. *Appl Phys A Mater Sci Process* 89:461–466
- Iwamoto S, Abe K, Yano H (2008) The effect of hemicellulose on wood pulp nanofibrillation and nanofiber network characteristics. *Biomacromolecules* 9(3):1022–1026
- Jiang F, Hsieh YL (2013) Chemically and mechanically isolated nanocellulose and their self-assembled structures. *Carbohydr Polym* 95(1):32–40
- Kajanto I, Kosonen M (2012) The potential use of micro- and nanofibrillated cellulose as a reinforcing element in paper. *J For* 2(6):42–48
- Lu Y, Tekinalp HL, Eberle CC, Peter W, Naskar AK, Ozcan S (2014) Nanocellulose in polymer composites and biomedical applications. *Tappi J* 13(6):47–54
- Marx-Figini M (1987) The acid-catalyzed degradation of cellulose linters in distinct ranges of degree of polymerization. *J Appl Polym Sci* 33(6):2097–2105
- Meng Q, Fu S, Lucia LA (2016) The role of heteropolysaccharides in developing oxidized cellulose nanofibrils. *Carbohydr Polym* 144:187–195
- Mohammadkazemi F, Doosthoseini K, Ganjian E, Azin M (2009) Manufacturing of bacterial nano-cellulose reinforced fiber-cement composites. *Constr Build Mater* 101:958–964
- Moran JL, Alvarez VA, Cyrus VP, Vazquez A (2008) Extraction of cellulose and preparation of nanocellulose from sisal fibers. *Cellulose* 15:149–159
- Nair SS, Yan N (2015) Effect of high residual lignin on the thermal stability of nanofibrils and its enhanced mechanical performance in aqueous environments. *Cellulose* 22:3137–3150
- Pääkkö M, Ankerfors M, Kosonen H, Nykänen A, Ahola S, Österberg M, Ruokolainen J, Laine J, Larsson PT, Ikkala O, Lindström T (2007) Enzymatic hydrolysis combined with mechanical shearing and high-pressure homogenization for nanoscale cellulose fibrils and strong gels. *Biomacromolecules* 8:1934–1941
- Puangsin B, Yanga Q, Saito T, Isogai A (2013) Comparative characterization of TEMPO-oxidized cellulose nanofibril films prepared from non-wood resource. *Int J Biol Macromol* 59:208–213
- Quiévy N, Jacquet N, Sclavons M, Deroanne C, Paquot M, Devaux J (2010) Influence of homogenization and drying on the thermal stability of microfibrillated cellulose. *Polym Degrad Stab* 95:165–188
- Rodríguez A, Sánchez R, Requejo A, Ferrer A (2010) Feasibility of rice straw as a raw material for the production of soda cellulose pulp. *J Clean Prod* 18:1084–1091
- Rouger J, Mutjé P (1984) Correlation between the cellulose fibers beating and the fixation of a soluble cationic polymer. *Br Polym J* 16(2):83–86
- Saito T, Isogai A (2004) TEMPO-mediated oxidation of native cellulose. The effect of oxidation conditions on chemical and crystal structures of the water-insoluble fractions. *Biomacromol* 5(5):1983–1989
- Saito T, Kimura S, Nishiyama Y, Isogai A (2007) Cellulose nanofibers prepared by TEMPO-mediated oxidation of native cellulose. *Biomacromolecules* 8:2485–2491
- Sánchez R, Espinosa E, Domínguez-Robles J, Loaiza JM, Rodríguez A (2016) Isolation and characterization of lignocellulose nanofibers from different wheat straw pulps. *Int J Biol Macromol* 92:1025–1033
- Segal L, Creely JJ, Martin AE, Conrad CM (1959) An empirical method for estimating the degree of crystallinity of native cellulose using X-ray diffractometer. *Text Res J* 29:786–794
- Sharma PR, Varma AJ (2014) Thermal stability of cellulose and their nanoparticles: effect of incremental increases in carboxyl and aldehyde groups. *Carbohydr Polym* 114:339–343
- Soni B, Hassan EB, Mahmoud B (2015) Chemical isolation and characterization of different cellulose nanofibers from cotton stalks. *Carbohydr Polym* 134:581–589
- Taipale T, Österberg M, Nykänen A, Ruokolainen J, Laine J (2010) Effect of microfibrillated cellulose and fines on the drainage of kraft pulp suspension and paper strength. *Cellulose* 17:1005–1020
- Tanaka R, Saito T, Isogai A (2012) Cellulose nanofibrils prepared from softwood cellulose by TEMPO/NaClO/NaClO₂ systems in water at pH 4.8 or 6.8. *Int J Biol Macromol* 51(3):228–234
- Tanaka R, Saito T, Ishii D, Isogai A (2014) Determination of nanocellulose fibril length by shear viscosity measurement. *Cellulose* 21:1581–1589
- Tarrés Q, Saguer E, Pèlach MA, Alcalá M, Delgado-Aguilar M, Mutjé P (2016) The feasibility of incorporating cellulose micro/nanofibers in papermaking processes: the relevance of enzymatic hydrolysis. *Cellulose* 23(2):1433–1445
- Tian C, Yi J, Wu Y, Wu Q, Qing Y, Wang L (2016) Preparation of highly charged cellulose nanofibrils using high-pressure homogenization coupled with strong acid hydrolysis pretreatments. *Carbohydr Polym* 136:485–492
- Turbak A, Snyder F, Sandberg K (1983) Microfibrillated cellulose: a new cellulose product: properties, uses, and commercial potential. *J Appl Polym Sci Appl Polym Symp* 37:815–827
- Vallejos ME, Felissia FE, Area MC, Ehman NV, Tarrés Q, Mutje P (2016) Nanofibrillated cellulose (CNF) from eucalyptus sawdust as a dry strength agent of unrefined eucalyptus handsheets. *Carbohydr Polym* 139:99–105
- Vargas F, González Z, Sánchez R, Jiménez L, Rodríguez A (2012) Cellulosic pulps of cereal straws as raw material for the manufacture of ecological packaging. *BioResources* 7(3):4161–4170
- Xiang Z, Gao W, Chen L, Lan W, Zhu JY, Runge T (2016) A comparison of cellulose nanofibrils produced from *Cladophora glomerata* algae and bleached eucalyptus pulp. *Cellulose* 23:493–503
- Xu Q, Gao Y, Qin M, Wu K, Fu Y, Zhao Y (2013) Nanocrystalline cellulose from aspen kraft pulp and its application in deinked pulp. *Int J Biol Macromol* 60:241–243
- Yousefi H, Faezipour M, Nishino T, Shakeri A, Ebrahimi G (2011) All-cellulose composite and nanocomposite made from partially dissolved micro and nanofibers of canola straw. *Polym J* 43:559–564